Farnesyltransferase Inhibitors Reverse Taxane Resistance

Adam I. Marcus,[1] Aurora M. O'Brate,[1] Ruben M. Buey,[2] Jun Zhou,[1,3] Shala Thomas,[1] Fadlo R. Khuri,[1] Jose Manuel Andreu,[2] Fernando Díaz,[2] and Paraskevi Giannakakou[1]

[1]Winship Cancer Institute, Emory University, Atlanta, Georgia; [2]Centro de Investigaciones Biológicas, Consejo Superior de Investigaciones Cientificas, Madrid, Spain; and [3]Department of Genetics and Cell Biology, Nankai University, Tianjin, China

Abstract

The combination of farnesyltransferase inhibitors (FTIs) and taxanes has been shown to result in potent antiproliferative and antimitotic synergy. Recent phase I and II clinical trials have shown that this combination shows clinical activity in taxane-refractory or taxane-resistant cancer patients. To understand the mechanism behind these clinical observations, we used a cancer cell model of paclitaxel resistance and showed that the FTI/taxane combination retains potent antiproliferative, antimitotic, and proapoptotic activity against the paclitaxel-resistant cells, at doses where each drug alone has little or no activity. To probe the mechanistic basis of these observations, paclitaxel activity was monitored in living cells using the fluorescently conjugated paclitaxel, Flutax-2. We observed that all FTIs tested increase the amount of microtubule-bound Flutax-2 and the number of microtubules labeled with Flutax-2 in both paclitaxel-resistant and paclitaxel-sensitive cells. Importantly, we observed a consequential increase in microtubule stability and tubulin acetylation with the combination of the two drugs, even in paclitaxel-resistant cells, confirming that the enhanced taxane binding in the presence of FTI affects microtubule function. Furthermore, this mechanism is dependent on the function of the tubulin deacetylase, HDAC6, because in cells overexpressing a catalytically inactive HDAC6, FTIs are incapable of enhancing Flutax-2–microtubule binding. Similar results were obtained by using an FTI devoid of farnesyltransferase inhibitory activity, indicating that functional inhibition of farnesyltransferase is also required. Overall, these studies provide a new insight into the functional relationship between HDAC6, farnesyltransferase, and microtubules, and support clinical data showing that the FTI/taxane combination is effective in taxane-refractory patients. (Cancer Res 2006; 66(17): 8838-46)

Introduction

The farnesyltransferase inhibitors (FTIs) are a novel class of targeted anticancer agents, originally designed to inhibit the function of Ras oncoproteins by preventing their farnesylation-dependent localization to the plasma membrane (1). However, mechanistic and clinical studies show that the anticancer activity of FTIs could not solely be attributed to Ras inhibition (2–4). Nevertheless, FTIs have shown modest activity in the clinic as single agents, whereas their combination with standard chemotherapy drugs has been promising (1). In particular, FTIs synergize with the microtubule-stabilizing drugs, paclitaxel and epothilones, in several *in vitro* and *in vivo* tumor models (5–8). However, the molecular mechanism underlying the FTI/taxane synergistic combination was largely unknown. Previous work from our laboratory has shed some insight into this mechanism, by showing that both *in vitro* and in cells, FTIs inhibit the tubulin deacetylase function of HDAC6, and in combination with taxanes they synergistically enhance tubulin acetylation (8). Because tubulin acetylation is associated with stable microtubules and taxanes bind preferentially to stabilized microtubules (9), we hypothesized that the FTI/taxane synergy is due to enhanced microtubule stability.

Interestingly, early clinical trials have shown clinical benefit of the FTI/taxane combination in patients refractory/resistant to a taxane alone (10, 11). This intriguing clinical result prompted us to test the FTI/taxane combination in a cell model of paclitaxel resistance, due to an acquired β-tubulin mutation at the binding site of the drug (12). Our results reveal that the FTI/taxane combination retains potent antiproliferative, antimitotic, and proapoptotic activity against paclitaxel-resistant cells, even at doses where taxanes or FTIs alone had little or no activity. To probe the mechanism behind these observations and to test our working hypothesis that FTIs enhance taxane binding to acetylated microtubules, we used live-cell microscopy to monitor the binding of a fluorescently conjugated paclitaxel (Flutax-2) to the microtubule. Our results revealed that the addition of FTIs, at doses that inhibit protein farnesylation, increased the levels of microtubule-bound Flutax-2 in the β-tubulin mutant, drug-resistant cells, compared with Flutax-2 alone (12, 13). Furthermore, this result was dependent on functional inhibition of the farnesyltransferase protein. In addition, functional inhibition of the tubulin deacetylase HDAC6, is also required for enhanced Flutax-2 binding to cellular microtubules. These results provide mechanistic insight into the functional relationship of farnesyltransferase, HDAC6, and microtubules, and can potentially affect the design of future clinical trials with a FTI/taxane combination in taxane-resistant/refractory patients.

Materials and Methods

Cell culture. Cell lines were maintained in RPMI 1640 supplemented with 5% fetal bovine serum and 1% penicillin/streptomycin. All lines were cultured at 37°C in a humidified atmosphere with 5% CO_2. The PTX10 paclitaxel-resistant cells were derived from 1A9 ovarian carcinoma cells as previously described (12).

Reagents. Lonafarnib (SCH66336) was provided by Schering Plough Research Institute (Kenilworth, NJ). FTI-277 was purchased from EMD Biosciences, Inc. (San Diego, CA). Both FTIs were dissolved in DMSO at a concentration of 10 mmol/L, and aliquots were stored at −80°C. Tubacin was a generous gift from Dr. Stuart Schreiber. Taxotere was a generous gift from Aventis Pharmaceuticals (Bridgewater, NJ), paclitaxel was

Note: A.I. Marcus and A.M. O'Brate contributed equally to this work.

Current address for A.M. O'Brate and P. Giannakakou: Weill Medical College of Cornell University, Division of Hematology and Medical Oncology, New York, NY 10021.

Requests for reprints: Paraskevi Giannakakou, Division of Hematology and Medical Oncology, Weill Cornell Medical College of Cornell University, 1300 York Avenue, Box 113, New York, NY 10021. Phone: 212-746-3783; Fax: 212-746-6731; E-mail: pag2015@med.cornell.edu.

doi:10.1158/0008-5472.CAN-06-0699

purchased from Sigma (St. Louis, MO), and vinblastine was from Calbiochem (San Diego, CA). Stock solutions were diluted to the desired final concentrations with growth medium just before use.

Cell proliferation and combination index analysis assays. The sulforhodamine B cytotoxicity assays was adapted from Skehan et al. (14) and was done as previously described (8). The combination index (CI) method described in Chou and Talalay (15) was used to determine the interaction between FTIs and taxanes, and the data was analyzed using Calcusyn software (Biosoft, Cambridge, United Kingdom). Briefly, the interaction of the two drugs (i.e., synergy, antagonism, or additivity) was determined by calculating the CI as a function of the fraction affected (100 − percentage cell survival / 100). A CI value >1 is antagonism, 1 is additivity, and <1 is synergy. Each CI value represents the mean ± SE of a least six independent experiments, whereby each data point was done in triplicate. To calculate *P* values determining if the CI value significantly differed from a CI of 1, one-sample *t* tests were done.

Immunofluorescence analysis. Immunofluorescence analysis of fixed cells followed by confocal microscopy was done as previously described (8). The following antibodies were used: α-tubulin antibody (Chemicon International, Temecula, CA) and Alexa 563–conjugated goat anti-mouse IgG (Molecular Probes, Eugene, OR). For DNA staining, we added Sytox Green (Molecular Probes) to the Gel Mount mounting medium (Biomeda Corp., Foster City, CA). The mitotic index was calculated by counting the number of mitotic cells after immunofluorescence staining for tubulin and DNA. For each drug treatment, ~300 cells were counted per experiment, and each experiment was done at least in triplicate. Cells in all phases of mitosis (prometaphase, metaphase, anaphase, and telophase) were counted and expressed as percentage of total cells.

Cell-based tubulin polymerization assay. Quantitative drug-induced tubulin polymerization was done as previously described (12). When vinblastine was used in this assay, the cells were lysed in a microtubule-stabilizing buffer [0.1 mol/L PIPES, 1 mmol/L EGTA, 1 mmol/L $MgSO_4$, 30% glycerol, 5% DMSO, 5 mmol/L GTP, 0.125% NP40, and protease inhibitors (pH 6.9)], instead of the low-salt buffer [20 mmol/L Tris-HCl, 1 mmol/L $MgCl_2$, 2 mmol/L EGTA, 0.125% NP40, and protease inhibitors (pH 6.8)] used with paclitaxel. The percent pellet (%*P*) is calculated as the amount of polymerized tubulin (*P*), over the total amount of polymerized and soluble tubulin (*P* + *S*) times 100, $\{P / (P + S) \times 100\}$, based on densitometry analysis. The blots were probed with an anti-α-tubulin antibody as described below.

Western blotting. Western blotting was done as previously described (8). The antibodies used were anti–poly(ADP-ribose)polymerase (PARP) p85 (Cell Signaling, Beverly, MA), anti-α-tubulin (Sigma), anti-HDJ-2 (Neomarkers, Fremont, CA), antiacetylated tubulin (Sigma), and anti-actin (Sigma).

Live-cell Flutax-2 binding studies. Cells were plated on live-cell imaging chambers from World Precision Instrument (Sarasota, FL) overnight. Before use, Flutax-2 (16, 17) was diluted to the proper concentration in medium and centrifuged at 14,000 rpm in an Eppendorf 5415C centrifuge for 10 minutes. Cells were treated with Flutax-2 or Flutax-2 + FTI for 16 hours at the doses indicated. After treatment, the cells were washed thrice in PBS and new medium was added to the cells. Cells were imaged using a Perkin-Elmer Ultraview ERS spinning disc confocal microscope. This system was mounted on a Zeiss Axiovert 200 m inverted microscope equipped with a 37°C stage warmer, incubator, and CO_2 perfusion. A ×63 or ×100 Zeiss oil objective (numerical aperture, 1.4) was used for all images and a Z-stack was created using the attached piezo electric z-stepper motor. The 488 nm laser line of an argon ion laser (set at 60% power) was used to excite the Flutax-2, and emission was detected with a Hamamatsu Orca-ER camera with exposure time from 200 to 400 ms. For each comparison, the exposure time and laser intensity was kept identical for accurate intensity measurement. Pixel intensity was quantitated using Metamorph 6.1 (Universal Imaging, Downingtown, PA) by first thresholding the image for filamentous microtubules and then calculating the mean pixel intensity using the Region Statistics feature on the software.

Flutax-2 binding assays. Chemicals, tubulin, and stabilized microtubules were generated as previously described (18). Deacetylation of stabilized microtubules was done by incubating cross-linked microtubules (200 μL of 6 μmol/L tubulin) in glycerol-containing assembly buffer (18) with the immunoprecipitates containing Flag-HDAC6-wild type (-wt) or Flag-HDAC6-mutant (-mut) on agarose beads (1 μL) prepared as described (19), for 2 hours at 37°C. Reaction mixtures were then placed on ice for 15 minutes and briefly centrifuged at 14,000 rpm to separate the supernatant, containing the deacetylated stabilized microtubules, from the agarose beads. The supernatant was then subjected to Western blotting using antiacetylated α-tubulin. Binding affinity constants of Flutax-2, a fluorescent analogue of paclitaxel, is well-characterized (16, 17). The binding affinity of Flutax-2 to stabilized deacetylated microtubules was measured by incubating 25 or 50 nmol/L of this ligand with increasing concentrations of microtubules (from 6 nmol/L to 1.2 μmol/L) at 25°C. The binding isotherms were measured several times in different plates by the anisotropy of the fluorescence using a fluorescence polarization microplate reader at 25°C. Fluorescence anisotropy was converted to fractional saturation as described (18) and data points were best fitted to the equation, $SF = K[x] / (1 + K[x])$, which describes the binding of a ligand to an unique site in a protein. *SF* is the fractional saturation and $[x]$ is the free ligand concentration.

Results

FTIs overcome drug resistance in taxane-resistant cancer cells. We have previously shown that the nonpeptidomimetic FTI, lonafarnib, synergizes with taxanes in a variety of human cancer cell lines by inhibiting the tubulin deacetylase activity of HDAC6 (8). These results were obtained using taxane-sensitive cancer cell lines and only one class of FTI (lonafarnib). Recent clinical studies (10, 11) showing efficacy of FTIs in taxane-refractory patients prompted us to investigate the effect of the FTI/taxane combination against paclitaxel-resistant cell lines. Our laboratory has established a model of paclitaxel resistance composed of the 1A9 drug-sensitive human ovarian carcinoma cell line and its derivative paclitaxel-resistant line, PTX10 (12). Paclitaxel resistance in this model is due to an acquired β-tubulin mutation (Fβ270V) at the drug binding site and results in ~25-fold resistance to paclitaxel and 10-fold cross-resistance to docetaxel. To investigate whether FTIs are active against these resistant cells, we determined the mean IC_{50} of FTIs and taxanes alone and in combination, in both 1A9 and PTX10 cells (Fig. 1*A*). These results showed that both FTIs tested (lonafarnib and the peptidomimetic FTI-277) retained activity against the drug-resistant PTX10 cells, as no significant differences in the mean IC_{50} values were obtained between the parental and resistant cell lines. Notably, the FTI/taxane combination resulted in a dramatic reversal of taxane resistance in PTX10 cells. Specifically, PTX10 cells, although exhibiting a 25-fold resistance to paclitaxel alone, were only 1.5-fold resistant to the lonafarnib/paclitaxel combination. Similar results were obtained with the FTI-277/paclitaxel combination, as well as the FTI combination with docetaxel (PTX10 cells are 10-fold cross-resistant docetaxel; Fig. 1*A*). It is also worth noting that a similar pattern was observed with the FTI tipifarnib (Johnson & Johnson, New Brunswick, NJ; data not shown).

To quantitate the extent of the synergistic interaction between the FTIs and the taxanes in the paclitaxel-resistant PTX10 cells, we used the CI analysis method (15). In this type of analysis, the fractional cell growth inhibition was plotted as a function of the CI, whereby a CI < 1 represents synergy, 1 is additivity, and >1 is antagonism. In the paclitaxel-sensitive 1A9 cells, all FTIs were synergistic with both paclitaxel and docetaxel (Fig. 1*B*; $P < 0.05$ for all), which is consistent with previous studies in other cell lines (5, 6, 8). In the paclitaxel-resistant PTX10 cells, we observed intermediate synergy when both FTIs were combined with paclitaxel (CI = 0.6-1.0) and their combination with docetaxel resulted in strong synergy in PTX10 cells (CI = 0.4-0.8; Fig. 1*B*). Thus, these

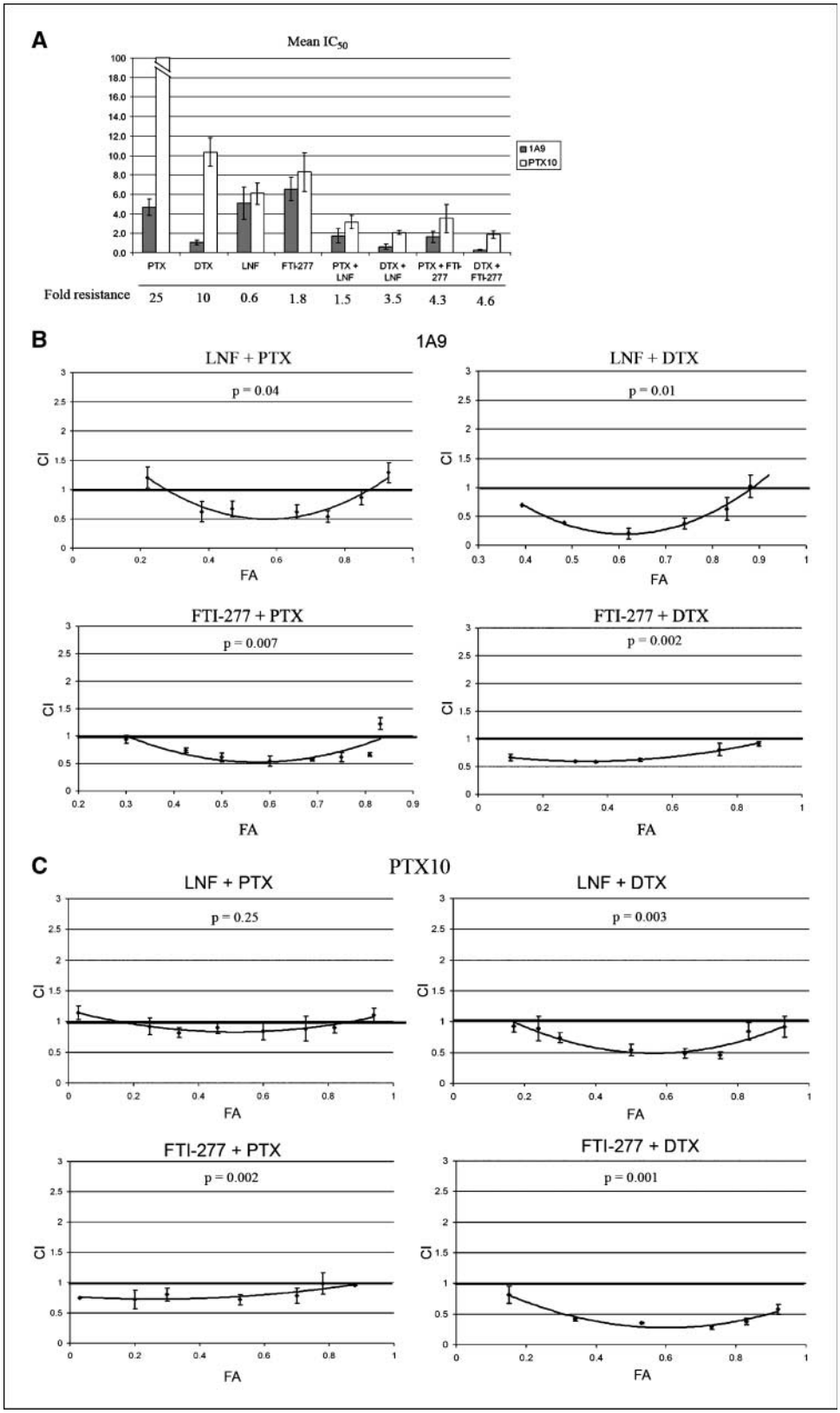

Figure 1. FTIs sensitize paclitaxel-resistant cancer cells to the effects of taxanes. *A,* mean IC_{50} values of the various drug treatments against the parental 1A9 and paclitaxel-resistant PTX10 cells. *Columns,* mean IC_{50} units, following a 72-hour drug exposure, are nmol/L for paclitaxel and docetaxel, and μmol/L for lonafarnib and FTI-277; *bars,* SE. *B* and *C,* CI analysis is plotted as a function of fractional cell growth inhibition (*FA*) in 1A9 paclitaxel-sensitive cells (*B*) and PTX10 paclitaxel-resistant cells (*C*). A CI >1 indicates antagonism, ~1 is additivity, and <1 is synergy. *Points,* mean CI values, representative of at least six independent experiments; *bars,* SE. A *P* value determining significance compared with a CI of 1 is also shown.

results are consistent with the data presented in Fig. 1*A* and confirm that the FTI/taxane combination can overcome drug resistance in taxane-resistant cancer cells. We also assessed the efficacy of the FTI (lonafarnib)/taxane combination in another cell model of paclitaxel resistance, the P-glycoprotein overexpressing A2780/AD10 cells, and their parental counterpart A2780 (20). We found that the FTI/taxane combination was synergistic in the presence and in the absence of the P-glycoprotein modulator verapamil (data

not shown). This result was expected as lonafarnib has been reported to be a P-glycoprotein inhibitor, similar to verapamil (21).

The FTI/taxane combination causes enhanced apoptosis and mitotic arrest in paclitaxel-resistant cells. To further confirm the FTI/taxane cytotoxic synergy in the paclitaxel-resistant cell lines, the effects of this drug combination on apoptosis was assayed using the cleaved form of PARP (p85) as a marker of apoptosis (Fig. 2*A*). Both 1A9 and PTX10 cells were subjected to various FTI/taxane treatments for 30 hours to allow sufficient time for apoptosis to occur. In the paclitaxel-sensitive 1A9 cells, the combination of either FTI (1 μmol/L) with low-dose paclitaxel (both 2 and 5 nmol/L) caused a dose-dependent increase of PARP cleavage compared with either FTI or paclitaxel alone (Fig. 2*A*). In the paclitaxel-resistant PTX10 cells, PARP cleavage was not induced with paclitaxel (5-50 nmol/L), consistent with the presence of the β-tubulin mutation at the drug binding site. However, upon addition of an FTI (1 μmol/L) to paclitaxel, significant PARP cleavage occurred, indicating that PTX10 cells were undergoing apoptosis due to the FTI/paclitaxel combination. Thus, the FTI/taxane combination causes enhanced apoptosis in both paclitaxel-resistant and paclitaxel-sensitive cells at doses where paclitaxel alone had little or no effect.

Paclitaxel is a potent antimitotic; however, in PTX10 cells, even high doses of paclitaxel lead to little or no mitotic arrest (22). To determine if the enhanced apoptosis induced by the FTI/paclitaxel combination in PTX10 cells was due to increased mitotic arrest, the mitotic index was determined in parental and drug-resistant cells using confocal microscopy (Fig. 2*B-C*). In 1A9 cells, the FTI/paclitaxel combination resulted in a potent increase in mitotic arrest (Fig. 2*B*; $P < 0.05$), which is consistent with our previous findings in other cell lines (8). In the drug-resistant PTX10 cells, high doses of paclitaxel (250 nmol/L) had minimal effect on mitotic arrest as expected; however, the FTI/paclitaxel combination retained its antimitotic activity, even at 2 nmol/L paclitaxel, indicating that the FTI/paclitaxel combination is an effective antimitotic combination in PTX10 paclitaxel-resistant cells (Fig. 2*C*). Taken together, these data show that although PTX10 cells do not undergo mitotic arrest with paclitaxel alone, the FTI/paclitaxel combination restores the antimitotic activity of paclitaxel.

FTIs increase Flutax-2 labeling of the microtubule. Our data thus far have shown that FTIs can restore the antiproliferative, antimitotic, and proapoptotic activity of the FTI/taxane combination in paclitaxel-resistant cells. Because PTX10 cells harbor a β-tubulin mutation at the paclitaxel binding site, we wanted to monitor the localization of paclitaxel in both paclitaxel-resistant and paclitaxel-sensitive cell lines to understand the mechanism behind these observations. We used live-cell confocal microscopy to localize the fluorescently conjugated paclitaxel molecule (Flutax-2; refs. 16, 17) in the paclitaxel-resistant PTX10 cells. Flutax-2 is ~100-fold less cytotoxic than unconjugated paclitaxel, due to the extra size added by the fluorophore; therefore, we used Flutax-2 concentrations equipotent to the low doses of paclitaxel used for each cell line in Fig. 2. In 1A9 drug-sensitive cells, 16-hour treatment with 75 nmol/L Flutax-2 alone resulted in a filamentous microtubule pattern (Fig. 3*A*), indicating that Flutax-2 was bound to microtubules. This low dose was chosen to prevent saturation of all taxoid-binding sites on the microtubule cytoskeleton with Flutax-2 alone, so that any enhancement due to lonafarnib activity would be more readily quantifiable. When we used a higher dose of Flutax-2 (1 μmol/L), we saw distinct microtubule bundling and disorganization of the microtubule cytoskeleton in 1A9 cells (data not shown). In contrast, little or no microtubule binding was observed in the drug-resistant PTX10 cells, even after treatment with a 10-fold higher concentration of Flutax-2 (750 nmol/L), reflecting the impaired ability of paclitaxel to bind microtubules in these β-tubulin mutant cells. Treatment of PTX10 cells with as high as 20 μmol/L Flutax-2 did not result in more extensive labeling of microtubules, but rather in diffuse Flutax-2 cytoplasmic accumulation (data not shown). When cells were coincubated with an FTI (lonafarnib or FTI-277) and Flutax-2, the intensity of Flutax-2 signal on the microtubule, as well as the number of Flutax-2-labeled microtubules, was significantly increased in both 1A9 and PTX10 cells (Fig. 3*A* and *B*). Thus, the addition of the FTI/Flutax-2 combination led to increased levels of Flutax-2 on the microtubule compared with Flutax-2 treatment alone.

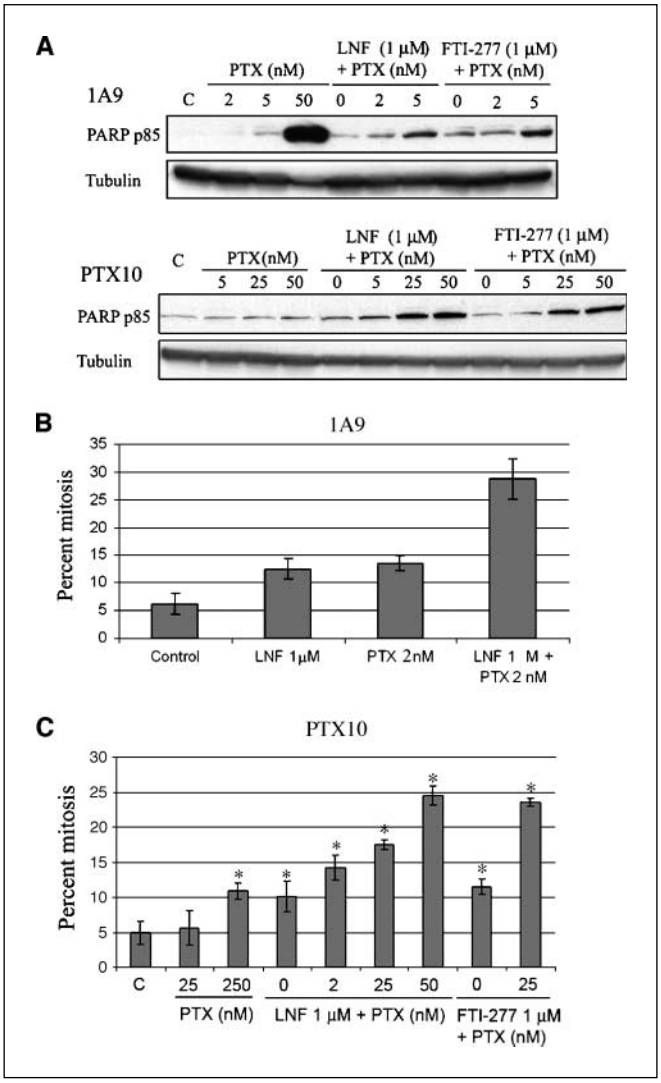

Figure 2. The FTI/paclitaxel combination enhances apoptosis and mitotic arrest in paclitaxel-sensitive and paclitaxel-resistant cells. *A,* Western blot assessing apoptosis using an antibody to cleaved PARP (p85). Both 1A9 (*top*) and PTX10 (*bottom*) cells were treated for 30 hours with varying doses of paclitaxel (*PTX*) and an FTI, both alone and in combination. *LNF,* lonafarnib. Tubulin is used as a protein loading control. *B,* percentage of 1A9 cells in mitosis after the various treatments for 16 hours. *Columns,* mean; *bars,* SE. *, $P < 0.05$, statistically significant from control. *C,* percentage of PTX10 cells in mitosis after the various treatments for 16 hours. *Columns,* mean; *bars,* SE. *, $P < 0.05$, statistically significant from control.

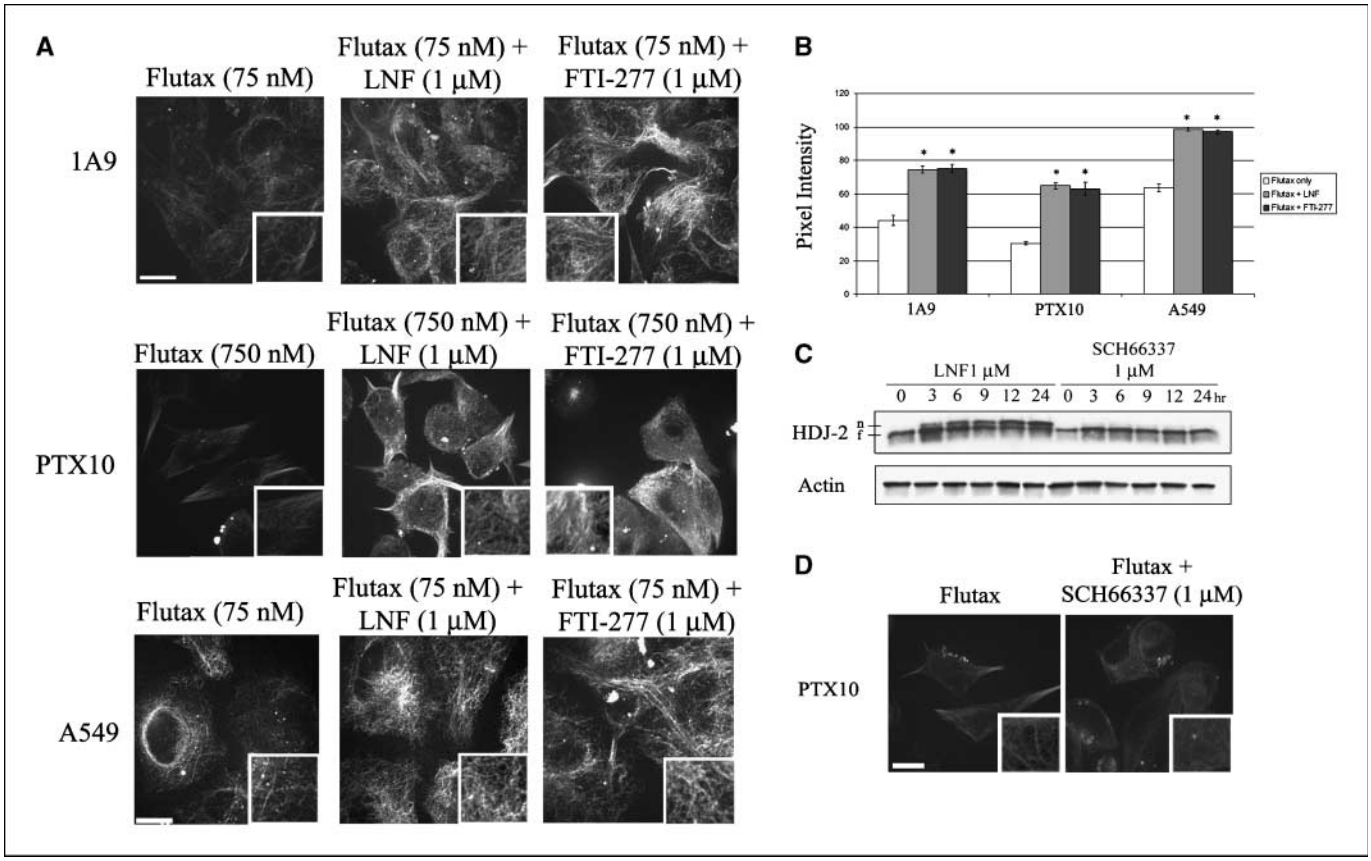

Figure 3. FTI treatment increases the affinity of Flutax-2 for the microtubule. *A,* live-cell imaging of Flutax-2 fluorescence in 1A9, PTX10, and A549 cells treated for 16 hours with the various drug combinations as indicated. Bar, 10 μm. *B,* average pixel intensity of at least 10 thresholded images of each cell line treated with Flutax-2 alone or Flutax-2 with an FTI. *Columns,* mean; *bars,* SE. *, $P < 0.05$, statistically significant from treatments with Flutax-2 alone. *C,* Western blot of HDJ-2 farnesylation. *Top band,* nonfarnesylated HDJ-2 (*n*); *bottom band,* farnesylated HDJ-2 (*f*). Actin is shown as a loading control. *D,* live-cell imaging of Flutax-2 fluorescence in PTX10 cells treated for 16 hours with either Flutax-2 alone (750 nmol/L) or Flutax-2 plus the inactive lonafarnib enantiomer, SCH66337 (1 μmol/L). Bar, 10 μm.

To determine if this scenario holds true in other cancer cell lines, a similar experiment was done in the lung cancer cell line, A549 (Fig. 3*A, bottom*). The combination of lonafarnib with Flutax-2 also resulted in a significant increase in Flutax-2 signal intensity and the number of Flutax-2-labeled microtubules in A549 cells, suggesting that the mechanism behind the FTI-induced enhancement of Flutax-2 on the microtubule may be conserved among different cancer cell lines.

Functional inhibition of farnesyltransferase is required for enhanced Flutax-2 labeling of microtubules. To investigate whether the FTI-induced enhancement of Flutax-2 binding on the microtubule is dependent on the inhibition of farnesyltransferase activity, we used the inactive lonafarnib enantiomer, SCH66337. This enantiomer is at least 100-fold less active than lonafarnib against farnesyltransferase *in vitro* and has practically no effect in cell systems (23). We first confirmed the lack of antifarnesyltransferase activity of SCH66337 by monitoring the drug-induced inhibition of protein farnesylation (HDJ-2 in this case) over time (Fig. 3*C*). As can be seen in Fig. 3*C*, lonafarnib (1 μmol/L) induced the nonfarnesylated, slower migrating HDJ-2 form as early as 3 hours posttreatment, whereas SCH66337 had no effect on HDJ-2 farnesylation even after 24 hours of treatment (Fig. 3*C*). Next, SCH66337 was used to determine if farnesyltransferase inhibition is required for the enhancement of Flutax-2 binding to the microtubule in PTX10 cells. Cells were treated for 16 hours with either Flutax-2 alone or Flutax-2 with SCH66337, and were monitored by live-cell confocal microscopy (Fig. 3*D*). In sharp contrast to our results with lonafarnib, SCH66337 did not result in increased Flutax-2 labeling of the microtubule, indicating that farnesyltransferase inhibition is required for the enhanced Flutax-2 microtubule labeling.

FTIs enhance tubulin acetylation and microtubule polymerization in paclitaxel-resistant cells. The results presented herein indicate that lonafarnib causes enhanced Flutax-2 interaction with microtubules in all cell lines tested, including paclitaxel-resistant cells. Paclitaxel binding to microtubules is known to increase microtubule polymerization and stabilization. Thus, FTI-induced Flutax-2 binding to microtubules should also affect these variables. To test this hypothesis, we used a cell-based microtubule polymerization assay to determine if FTI-induced paclitaxel binding leads to an enhancement of microtubule polymer mass. This quantitative tubulin polymerization assay (12) is based on the principle that polymerized microtubules remain detergent insoluble when extracted in a hypotonic buffer, and therefore are found in the pellet after centrifugation, whereas soluble nonpolymerized tubulin remains in the supernatant. In paclitaxel-sensitive 1A9 cells (Fig. 4*A*), the combination of lonafarnib with low-dose paclitaxel (2 nmol/L) caused a large increase in the percentage of stable polymerized tubulin found in the pellet relative to either drug alone (compare 48% of lonafarnib/paclitaxel 2 nmol/L with 9% of paclitaxel 2 nmol/L alone). Importantly, a similar result was

observed in the paclitaxel-resistant PTX10 cells (Fig. 4*B*), whereby paclitaxel alone had no effect on tubulin polymerization, but the combination of lonafarnib with only 10 nmol/L paclitaxel led to 37% of tubulin found in the pellet; on the other hand, almost half of the total tubulin was polymerized when 100 nmol/L paclitaxel was combined with lonafarnib, in sharp contrast to the 20% tubulin polymerization achieved with paclitaxel 100 nmol/L alone. An even more pronounced effect of the paclitaxel/lonafarnib drug combination was observed on the relative distribution of acetylated tubulin (Fig. 4*A* and *B*). Tubulin acetylation is a posttranslational modification (at lysine 40 of α-tubulin), occurring on the microtubule polymer, and serves as a hallmark of stable microtubules (24). To further corroborate these results, Western blotting for total acetylated tubulin in cell lysates from 1A9 and PTX10 cells was done (Fig. 4*C*). As a positive control for tubulin acetylation, cells were treated with tubacin, which increases tubulin acetylation levels by inhibiting the tubulin deacetylase HDAC6 (25, 26). Our results show that the lonafarnib/paclitaxel combination resulted in a synergistic increase in tubulin acetylation in both 1A9 and PTX10 cells, compared with either drug alone.

Because paclitaxel treatment alone is known to stabilize microtubules, in the experiments where paclitaxel is used together with lonafarnib, it is difficult to dissect whether lonafarnib alone–induced tubulin acetylation can confer microtubule stability. To test this hypothesis, we assessed the ability of the microtubule-destabilizing drug vinblastine to depolymerize microtubules in A549 cells pretreated with 5 μmol/L lonafarnib overnight (Fig. 4*D*). As shown in the figure, a dose-dependent microtubule depolymerization was observed when cells were exposed to vinblastine alone for 6 hours. In contrast, lonafarnib treatment protected microtubules from vinblastine-induced depolymerization. For example, in cells pretreated with lonafarnib, 85% of total tubulin was still polymerized (% pellet) following treatment with 10 nmol/L vinblastine, in contrast to 23% of polymerized tubulin with 10 nmol/L of vinblastine alone. Even at the highest dose (250 nmol/L vinblastine), which by itself caused almost complete depolymerization (3% in the pellet), lonafarnib protected microtubules against destabilization as seen by the remaining 31% of stabilized tubulin in the pellet. Consistent with all of our previous data, lonafarnib treatment (at time 0, before the 6-hour vinblastine treatment) resulted in increased tubulin acetylation (data not shown).

Taken together, these data provide further evidence that combination of lonafarnib with paclitaxel synergistically increases microtubule stability in both paclitaxel-sensitive and paclitaxel-resistant cell lines.

Functional HDAC6 is required for FTI-enhanced Flutax-2 binding to cellular microtubules. As we have previously shown that functional HDAC6 is required for lonafarnib/taxane synergy (8), we sought to determine if functional HDAC6 is required for the ability of lonafarnib to enhance the extent of Flutax-2 labeling of microtubules. To do this, we used NIH-3T3 cells stably expressing wild-type HDAC6 or a mutant catalytically inactive HDAC6 (19). In the HDAC6-mut cell line, the tubulin deacetylase function of HDAC6 is compromised resulting in higher basal levels of acetylated tubulin compared with the HDAC6-wt cells (8, 19). In this experiment, both HDAC6-wt and HDAC6-mut cell lines were treated with either Flutax-2 alone or the lonafarnib/Flutax-2 combination. When lonafarnib was combined with Flutax-2 in the HDAC6-wt cells, there was a significant increase in microtubule-bound Flutax-2 (Fig. 5*A*), as observed with other cell lines (Fig. 3).

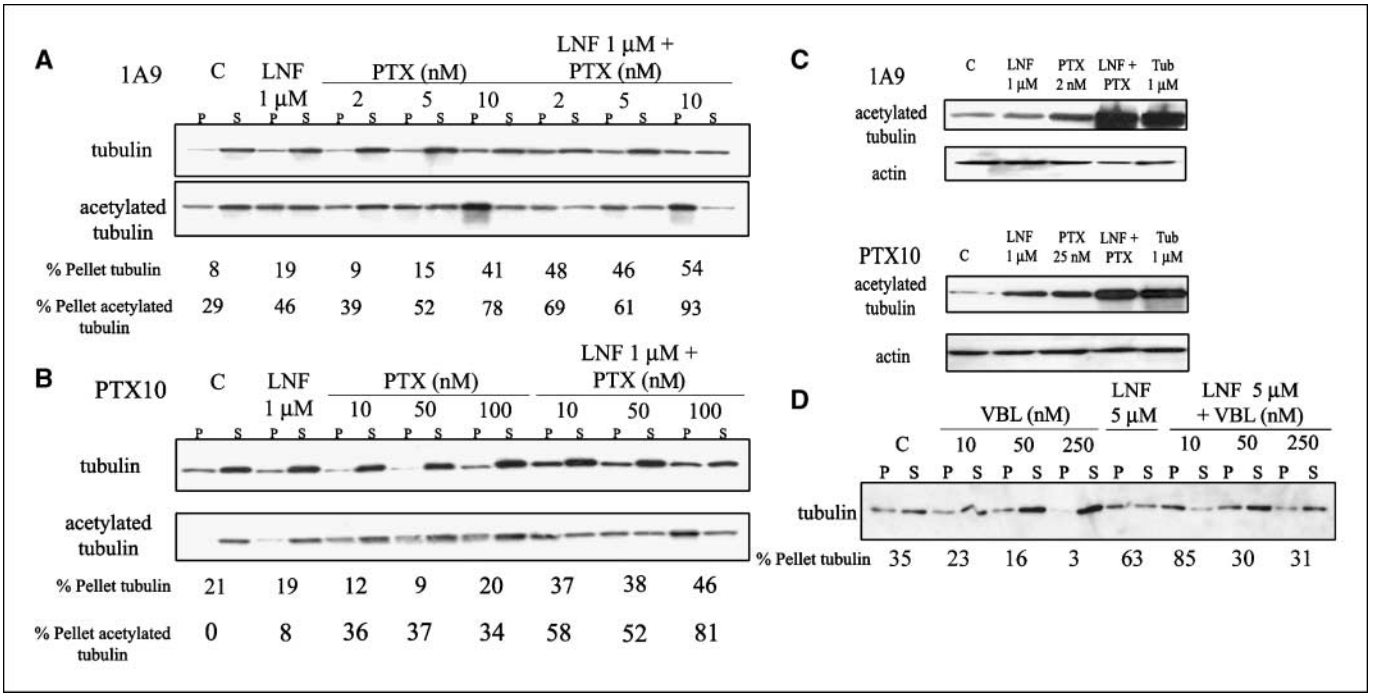

Figure 4. Microtubule polymerization/stability assays in 1A9, PTX10, and A549 cells. 1A9 (*A*) and PTX10 (*B*) cells were treated with the indicated drug combinations overnight. At the end of drug treatment, cells were lysed with a hypotonic buffer and microtubule polymers (*P*) were separated from soluble tubulin (*S*) via centrifugation, resolved by SDS-PAGE, and immunoblotted for total tubulin and acetylated tubulin. The percentage of tubulin and acetylated tubulin in the pellet fractions was quantitated by densitometry. *C,* acetylated tubulin immunoblot of whole cell lysates from 1A9 and PTX10 cells treated overnight as indicated. *Tub,* tubacin. Actin is shown as a loading control. *D,* A549 cells were pretreated with 5 μmol/L lonafarnib overnight (where indicated) followed by a 6-hour treatment with various vinblastine (*VBL*) concentrations. Cells were lysed with a glycerol-containing buffer and microtubule polymers (*P*) were separated from soluble tubulin (*S*) via centrifugation, resolved by SDS-PAGE, and immunoblotted for total tubulin. The percentage of polymerized tubulin (%pellet) was quantitated by densitometry.

However, in contrast to any other cell line tested, the addition of lonafarnib had no effect on microtubule-bound Flutax-2 (Fig. 5*A* and *B*) in the HDAC6-mut cells; that is, a greater fluorescent intensity signal was not observed nor a greater number of Flutax-2-labeled microtubules were present. Because these cell lines only differ in the functional status of HDAC6, these results show that HDAC6 is required for the ability of lonafarnib to enhance the microtubule-stabilizing effects of fluorescent paclitaxel and support our previous data indicating that a functional HDAC6 is required for lonafarnib/paclitaxel synergy (8).

Flutax-2 has a similar affinity for acetylated and deacetylated microtubules *in vitro*. To further examine the effect of HDAC6 function and tubulin acetylation on paclitaxel binding, we did a series of *in vitro* paclitaxel-binding experiments, using the fluorescent paclitaxel analogue Flutax-2 (17, 27, 28). These experiments are designed to address the question of whether Flutax-2 has a greater affinity for acetylated microtubules relative to deacetylated microtubules *in vitro*. For this assay, we obtained stabilized/acetylated microtubules by cross-linking purified microtubules with glutaraldehyde. Then, these microtubules were deacetylated *in vitro* by the addition of immunoprecipitated HDAC6-wt. Before the Flutax-2-binding assays, we confirmed the acetylation status of the purified microtubules by using Western blot analysis (Fig. 5*C*). As shown in duplicate, incubation of the microtubules with HDAC6-wt cell immunoprecipitates (WT1 and WT2) reduced tubulin acetylation *in vitro* relative to control glutaraldehyde cross-linked microtubules (C1 and C2). Furthermore, incubation of microtubules with HDAC6-mut (a catalytically inactive HDAC6; ref. 19) cell immunoprecipitates (MUT1 and MUT2) had no effect on tubulin acetylation *in vitro*. Thus, this *in vitro* microtubule deacetylation system accurately reflects the known tubulin deacetylation properties of HDAC6. To determine if Flutax-2 has a greater affinity for acetylated microtubules compared with deacetylated microtubules, the K_a of Flutax-2 was determined for each experimental condition (Fig. 5*D*). The K_a of Flutax-2 for microtubules deacetylated by HDAC6-wt was 94.4 $\pm$ 3.6% of that obtained for control microtubules, whereas microtubules treated with HDAC6-mut were 109.9 $\pm$ 4.1% of control microtubules (Fig. 5*D*). Although there is a small difference in the binding affinity of Flutax-2 to deacetylated microtubules compared with acetylated microtubules, this *in vitro* data cannot fully explain the marked differences seen with Flutax-2 binding to cellular microtubules, suggesting that other cellular components may contribute to this mechanism.

Discussion

The FTI/taxane combination has shown potent antiproliferative synergy in cell lines and preclinical models (5–7). Results from a phase I (10) and phase II clinical trial (11) in solid tumors showed that a subset of patients previously refractory/resistant to taxane therapy still responded to lonafarnib/paclitaxel combination, suggesting that the combination of paclitaxel with an FTI may reverse clinical drug resistance. Our data supports this hypothesis and shows that in paclitaxel-resistant cells, the FTI/taxane combination retains potent antiproliferative, antimitotic, and proapoptotic activity (Figs. 1 and 2). This effect seems to be due to enhanced binding of paclitaxel, visually evidenced through Flutax-2 (fluorescently conjugated paclitaxel) binding to the microtubule, in both paclitaxel-sensitive and paclitaxel-resistant ovarian carcinoma cell lines in the presence of an FTI (Fig. 3). This enhanced drug binding is associated with an increase in tubulin acetylation and microtubule polymer mass (Fig. 4*A* and *B*), both of which are hallmarks of paclitaxel efficacy. Furthermore, this effect is HDAC-6 dependent (Fig. 5) in accordance with our previous data showing that the combination of lonafarnib and paclitaxel inhibits HDAC6 activity *in vitro*, leading to increased tubulin acetylation (8).

In addition, functional inhibition of farnesyltransferase seems to be required as the inactive lonafarnib enantiomer, incapable of binding and inhibiting farnesyltransferase *in vitro*, did not potentiate paclitaxel binding on the microtubule (Fig. 3*D*). This result is intriguing as neither tubulin, nor any of the known microtubule-associated proteins, nor HDAC6 contain any

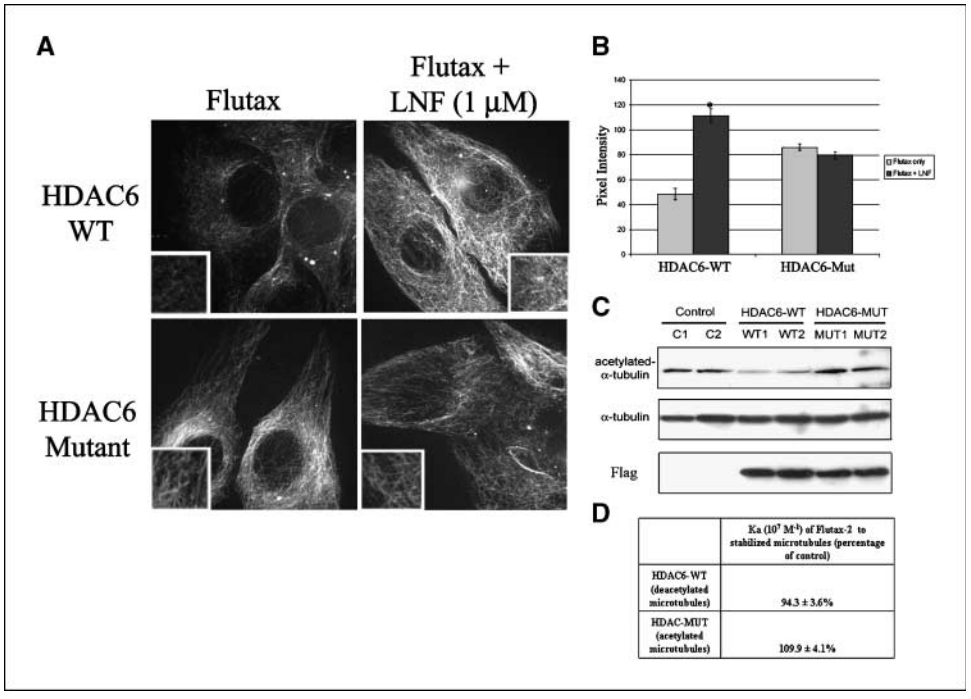

Figure 5. HDAC6 functionality is required for FTIs to enhance the affinity of paclitaxel for the microtubule. *A,* live-cell imaging of Flutax-2 fluorescence in HDAC6-wt and HDAC6-mut cell lines. Cells were treated for 16 hours with Flutax-2 alone (75 nmol/L; *left*) or Flutax-2 (75 nmol/L) plus lonafarnib (1 μmol/L; *right*). *B,* average pixel intensity of each cell line treated with Flutax-2 alone or Flutax-2 and lonafarnib. *Columns,* means; *bars,* SE. *, $P < 0.05$, statistically significant from treatments with Flutax-2 alone. *C,* Western blots of acetylated tubulin were done in duplicate on stabilized microtubules incubated with beads only (C1 and C2), FLAG-HDAC6-wt (WT1 and WT2) beads, and FLAG-HDAC6-mut (MUT1 and MUT2) beads. Total tubulin is shown as a control. The blots were also probed for FLAG to confirm the presence of the various FLAG-tagged WT-HDAC and HDAC6-mut proteins. *D,* binding affinity constants of Flutax-2 to stabilized microtubules in the presence of HDAC6-wt beads, HDAC6-mut beads, and beads alone. Data are the average values of six independent measurements with the respective SE.

consensus farnesyltransferase targeting motif (CAAX). Hence, what is the role of farnesyltransferase in the regulation of microtubule stability and acetylation through HDAC6 inhibition? Potentially, farnesyltransferase could regulate HDAC6 function in a farnesylation-independent manner, similar to the proposed interaction of farnesyltransferase and the TβR-I kinase domain of the transforming growth factor-β (29). However, this is unlikely given our results with the inactive lonafarnib enantiomer, SCH66337, as well as our data showing that this mechanism is shared by all classes of FTIs. Therefore, a strong possibility is that an upstream farnesylation event could modulate HDAC6 activity (leading to enhanced microtubule acetylation) and increase microtubule stability. An alternative possibility is that our proposed mechanism is farnesylation independent but does require inhibition of a novel function of farnesyltransferase. This novel function could be inhibited by a change in the protein conformation following binding of an FTI (hence, the results with the nonfarnesyltransferase binding inactive lonafarnib enantiomer).

In our working model of FTI-induced taxane binding on the microtubule, the central component is enhanced microtubule stability, presumably through HDAC6 inhibition leading to enhanced tubulin acetylation. However, it is still controversial in the literature as to whether tubulin acetylation is just a posttranslational modification "marking" stable, long-lived, less-dynamic microtubules, or whether tubulin acetylation leads to enhanced microtubule stability (19, 24, 30, 31). To investigate whether the enhanced tubulin acetylation we have been consistently observing following FTI treatment (Fig. 4; ref. 8) confers microtubule stability, we examined the effects of lonafarnib on vinblastine-induced microtubule depolymerization. Our results clearly show that lonafarnib treatment protects microtubules against vinblastine-induced destabilization, suggesting that acetylated lonafarnib-treated microtubules are indeed more stable (Fig. 4*D*). In a separate experiment, we have also observed that lonafarnib treatment protects microtubules against cold-induced destabilization, in a time-dependent manner (data not shown), further supporting our previous conclusion. Furthermore, according to our working model, the increased microtubule stability induced by lonafarnib should confer resistance to microtubule-depolymerizing drugs. To this end, we combined lonafarnib with vinblastine in a cytotoxicity assay similar to the experiments described in Fig. 1 and assessed the efficacy of the drug combination using the CI analysis. Our results revealed that the lonafarnib/vinblastine combination was antagonistic (CI = 2; data not shown). This result corroborates our working hypothesis and is consistent with published data showing that FTIs are synergistic with microtubule-stabilizing drugs but not with destabilizing ones (5).

Importantly, our data show that FTIs can overcome taxane resistance in PTX10 cells by enhancing Flutax-2-microtubule labeling, indicating enhanced drug-tubulin interaction. This result raises the question of how this enhanced interaction can be compatible with the presence of the tubulin mutation (Fβ270V) at the taxane-binding site in these cells. It is possible that because paclitaxel is known to have a greater affinity for the microtubule polymer (9, 32), and FTIs induce microtubule polymer formation (ref. 8; by affecting tubulin acetylation/stabilization and microtubule network formation; ref. 33), then the FTI-induced polymer formation would lead to a larger amount of microtubule taxoid binding sites, thereby enabling a larger number of paclitaxel molecules to bind microtubules even in the PTX10 paclitaxel-resistant cells. This result is also consistent with our previous data in PTX10 cells showing that although the acquired β-tubulin mutation (Fβ270V) is located at the taxane binding pocket, it significantly impairs but does not completely prevent paclitaxel binding to tubulin. Indeed, when the mutant tubulin was purified from the PTX10 cells for an *in vitro* tubulin polymerization assay, we observed that paclitaxel was still able to induce a certain amount of mutant tubulin polymerization (12), albeit at a fraction of wild-type tubulin, suggesting that the affinity of paclitaxel for the mutant tubulin was not entirely abolished but rather significantly reduced. Furthermore, considering that paclitaxel binds microtubules *in vitro* with a 1:1 stoichiometry (9, 32), but in cells as little as one paclitaxel molecule bound per every 400 tubulin dimers is enough to exert cellular/cytotoxic effects, the observed enhanced labeling of Flutax-2 microtubules in the resistant cells may be sufficient for paclitaxel to exert its microtubule-stabilizing and antimitotic activity, even within the drug resistance milieu.

Our results strongly favor a model centered on the effects of FTIs on interphase microtubules, which requires both functional HDAC6 as well as functional inhibition of farnesyltransferase. However, the exact mechanism by which FTIs exert their effects on microtubules in cells still remains unclear. We have recently shown that the FTI lonafarnib does not promote or modulate tubulin assembly *in vitro*, using purified tubulin with and without microtubule-associated proteins (34). This *in vitro* result is in sharp contrast to the observed effects of lonafarnib on cellular microtubules, suggesting that any microtubule-stabilizing activity of lonafarnib (i.e., tubulin acetylation, suppression of microtubule dynamics, and increase in polymer formation) would come from the interaction of lonafarnib and its target farnesyltransferase, with other factors in signaling pathways that may be regulating microtubule stability in addition to HDAC6.

Although the precise mechanism by which the FTI/taxane combination synergizes and overcomes drug resistance is not entirely clear, our results support clinical data showing that the FTI/taxane combination is effective in paclitaxel-resistant cells and can potentially affect the design of future clinical trials in taxane-resistant/refractory patients. The mechanism by which taxane resistance occurs in the clinic is still under debate (35, 36); however, overcoming taxane resistance by adding an FTI could prove useful in the treatment of several solid tumors. Still, another challenge would be to determine in which patients this treatment would prove beneficial; thus, future experiments will focus on determining which molecular markers (e.g., HDAC6 and acetylated tubulin) could predict response to drug treatment with the FTI/taxane combination. Overall, these results provide a putative mechanism of synergy between FTIs and taxanes in both paclitaxel-resistant and paclitaxel-sensitive cancer cells. Thus, FTIs in combination with taxanes may prove to be a beneficial chemotherapeutic strategy, especially in patients resistant/refractory to paclitaxel alone.

Acknowledgments

Received 2/28/2006; revised 5/26/2006; accepted 6/15/2006.

Grant support: NIH grants CA114335 and CA100202-04, Aventis Pharmaceuticals, Lung PO1 seed grant (P. Giannakakou), and MECD-FPU predoctoral fellowship (R.M. Buey).

The costs of publication of this article were defrayed in part by the payment of page charges. This article must therefore be hereby marked *advertisement* in accordance with 18 U.S.C. Section 1734 solely to indicate this fact.

We thank the Winship Cancer Institute Cell Imaging and Microscopy Core for their service and support, T.P. Yao (Duke University, Durham, NC) for providing us with the HDAC6-wt and HDAC6-mut NIH-3T3 cells, and Dr. Stuart Schreiber (Harvard University, Cambridge, MA) for tubacin.

References

1. Adjei AA. An overview of farnesyltransferase inhibitors and their role in lung cancer therapy. Lung Cancer 2003; 41 Suppl 1:S55–62.
2. End DW, Smets G, Todd AV, et al. Characterization of the antitumor effects of the selective farnesyl protein transferase inhibitor R115777 *in vivo* and *in vitro*. Cancer Res 2001;61:131–7.
3. Nagasu T, Yoshimatsu K, Rowell C, Lewis MD, Garcia AM. Inhibition of human tumor xenograft growth by treatment with the farnesyl transferase inhibitor B956. Cancer Res 1995;55:5310–4.
4. Sepp-Lorenzino L, Ma Z, Rands E, et al. A peptidomimetic inhibitor of farnesyl: protein transferase blocks the anchorage-dependent and -independent growth of human tumor cell lines. Cancer Res 1995;55:5302–9.
5. Moasser MM, Sepp-Lorenzino L, Kohl NE, et al. Farnesyl transferase inhibitors cause enhanced mitotic sensitivity to Taxol and epothilones. Proc Natl Acad Sci U S A 1998;95:1369–74.
6. Shi B, Yaremko B, Hajian G, et al. The farnesyl protein transferase inhibitor SCH66336 synergizes with taxanes *in vitro* and enhances their antitumor activity *in vivo*. Cancer Chemother Pharmacol 2000;46:387–93.
7. Sun J, Blaskovich MA, Knowles D, et al. Antitumor efficacy of a novel class of non-thiol-containing peptidomimetic inhibitors of farnesyltransferase and geranylgeranyltransferase I: combination therapy with the cytotoxic agents cisplatin, Taxol, and gemcitabine. Cancer Res 1999;59:4919–26.
8. Marcus AI, Zhou J, O'Brate A, et al. The synergistic combination of the farnesyl transferase inhibitor lonafarnib and paclitaxel enhances tubulin acetylation and requires a functional tubulin deacetylase. Cancer Res 2005;65:3883–93.
9. Schiff PB, Fant J, Horwitz SB. Promotion of microtubule assembly *in vitro* by Taxol. Nature 1979;277:665–7.
10. Khuri FR, Glisson BS, Kim ES, et al. Phase I study of the farnesyltransferase inhibitor lonafarnib with paclitaxel in solid tumors. Clin Cancer Res 2004;10: 2968–76.
11. Kim ES, Kies MS, Fossella FV, et al. Phase II study of the farnesyltransferase inhibitor lonafarnib with paclitaxel in patients with taxane-refractory/resistant non-small cell lung carcinoma. Cancer 2005;104:561–9.
12. Giannakakou P, Sackett DL, Kang YK, et al. Paclitaxel-resistant human ovarian cancer cells have mutant β-tubulins that exhibit impaired paclitaxel-driven polymerization. J Biol Chem 1997;272:17118–25.
13. Nogales E, Whittaker M, Milligan RA, Downing KH. High-resolution model of the microtubule. Cell 1999;96: 79–88.
14. Skehan P, Storeng R, Scudiero D, et al. New colorimetric cytotoxicity assay for anticancer-drug screening. J Natl Cancer Inst 1990;82:1107–12.
15. Chou TC, Talalay P. Quantitative analysis of dose-effect relationships: the combined effects of multiple drugs or enzyme inhibitors. Adv Enzyme Regul 1984;22: 27–55.
16. Evangelio JA, Abal M, Barasoain I, et al. Fluorescent taxoids as probes of the microtubule cytoskeleton. Cell Motil Cytoskeleton 1998;39:73–90.
17. Diaz JF, Strobe R, Engelborghs Y, Souto AA, Andreu JM. Molecular recognition of Taxol by microtubules. Kinetics and thermodynamics of binding of fluorescent Taxol derivatives to an exposed site. J Biol Chem 2000; 275:26265–76.
18. Buey RM, Diaz JF, Andreu JM, et al. Interaction of epothilone analogs with the paclitaxel binding site: relationship between binding affinity, microtubule stabilization, and cytotoxicity. Chem Biol 2004;11:225–36.
19. Hubbert C, Guardiola A, Shao R, et al. HDAC6 is a microtubule-associated deacetylase. Nature 2002;417: 455–8.
20. Naito M, Oh-hara T, Yamazaki A, Danki T, Tsuruo T. Reversal of multidrug resistance by an immunosuppressive agent FK-506. Cancer Chemother Pharmacol 1992; 29:195–200.
21. Wang EJ, Johnson WW. The farnesyl protein transferase inhibitor lonafarnib (SCH66336) is an inhibitor of multidrug resistance proteins 1 and 2. Chemotherapy 2003;49:303–8.
22. Zhou J, O'Brate A, Zelnak A, Giannakakou P. Survivin deregulation in β-tubulin mutant ovarian cancer cells underlies their compromised mitotic response to Taxol. Cancer Res 2004;64:8708–14.
23. Njoroge FG, Vibulbhan B, Rane DF, et al. Structure-activity relationship of 3-substituted *N*-(pyridinylacetyl)-4-(8-chloro-5,6-dihydro-11*H*-benzo[5,6]cyclohepta[1,2-*b*] pyridine-11-ylidene)-piperidine inhibitors of farnesyl-protein transferase: design and synthesis of *in vivo* active antitumor compounds. J Med Chem 1997;40:4290–301.
24. Westermann S, Weber K. Post-translational modifications regulate microtubule function. Nat Rev Mol Cell Biol 2003;4:938–47.
25. Haggarty SJ, Koeller KM, Wong JC, Grozinger CM, Schreiber SL. Domain-selective small-molecule inhibitor of histone deacetylase 6 (HDAC6)-mediated tubulin deacetylation. Proc Natl Acad Sci U S A 2003;100: 4389–94.
26. Hideshima T, Bradner JE, Wong J, et al. Small-molecule inhibition of proteasome and aggresome function induces synergistic antitumor activity in multiple myeloma. Proc Natl Acad Sci U S A 2005;102: 8567–72.
27. Diaz JF, Barasoain I, Souto AA, Amat-Guerri F, Andreu JM. Macromolecular accessibility of fluorescent taxoids bound at a paclitaxel binding site in the microtubule surface. J Biol Chem 2005;280:3928–37.
28. Diaz JF, Barasoain I, Andreu JM. Fast kinetics of Taxol binding to microtubules. Effects of solution variables and microtubule-associated proteins. J Biol Chem 2003; 278:8407–19.
29. Ventura F, Liu F, Doody J, Massague J. Interaction of transforming growth factor-β receptor I with farnesyl-protein transferase-α in yeast and mammalian cells. J Biol Chem 1996;271:13931–4.
30. Matsuyama A, Shimazu T, Sumida Y, et al. *In vivo* destabilization of dynamic microtubules by HDAC6-mediated deacetylation. EMBO J 2002;21:6820–31.
31. Palazzo A, Ackerman B, Gundersen GG. Cell biology: tubulin acetylation and cell motility. Nature 2003;421:230.
32. Diaz JF, Andreu JM. Assembly of purified GDP-tubulin into microtubules induced by Taxol and taxotere: reversibility, ligand stoichiometry, and competition. Biochemistry 1993;32:2747–55.
33. Suzuki N, Del Villar K, Tamanoi F. Farnesyltransferase inhibitors induce dramatic morphological changes of KNRK cells that are blocked by microtubule interfering agents. Proc Natl Acad Sci U S A 1998;95: 10499–504.
34. Buey RM, Barasoain I, Jackson E, et al. Microtubule interactions with chemically diverse stabilizing agents: thermodynamics of binding to the paclitaxel site predicts cytotoxicity. Chem Biol 2005;12:1269–79.
35. Orr GA, Verdier-Pinard P, McDaid H, Horwitz SB. Mechanisms of Taxol resistance related to microtubules. Oncogene 2003;22:7280–95.
36. Jordan MA, Wilson L. Microtubules as a target for anticancer drugs. Nat Rev Cancer 2004;4:253–65.